JOURNAL OF MATERIALS SCIENCE 33 (1998) 3629–3637

On the creep rupture life prediction

A. BALDAN
Department of Mechanical Engineering, Mersin University, Çiftlikköy, Mersin, Turkey

Combined effects of stress, σ_A, and fracture cavitation on the creep rupture life, t_R, have been studied in conventionally cast MAR-M 002 alloy tested at 1173 K (900 °C) over a limited range of stress ($\sigma_A = 200$–400 MPa). It is predicted that the creep fracture cavity growth is controlled by the coupled power-law creep with the grain-boundary diffusion mechanism. On the basis of this prediction the Edward–Ashby model overestimates the creep rupture life although this model correctly describes the trend in the data. The observation of a linearity between the cavity density, N_A, and the product $\varepsilon_R t_R \sigma_A^4$ indicates that this relationship can be used to predict the creep time, t_R, where ε_R is the rupture strain. Furthermore, another empirical method is the creep-fracture parameter, $K_f = \sigma_f(\pi a_c)^{1/2}$, approach, developed using the modified Griffith–Irwin type of relationship, which can also be used to predict the creep rupture life in the present alloy, where σ_f is the creep fracture stress (or the applied stress, σ_A) and a_c the crack (or cavity) size.

1. Introduction

Under high-temperature creep conditions, fracture usually occurs in an intergranular manner by the nucleation, growth and link-up of grain-boundary (GB) cavities which leads to the crack formation. The modelling of the growth of intergranular cavities during creep has attracted considerable attention in the last 20 years [1–5]. Creep cavitation can grow by mechanisms controlled by GB diffusion, by surface diffusion, by power-law creep (PLC), and by any combination of two of these mechanisms. The problem of coupling diffusive cavity growth with PLC has been analysed by Beere and Speight [1], Edward and Ashby [2], Needleman and Rice [3] and Chen and Argon [4]. It was suggested that the GB area between cavities should be divided into two regions: one which is adjacent to the cavities where GB diffusion occurs, and the other which is midway between the cavities where PLC occurs.

During the creep of nickel-based superalloys at elevated temperatures a number of micromechanistic processes (i.e., γ' coarsening, grain structure, segregation, microporosity, cavitation on the GB carbides, etc.) occurs which damage the structural integrity of the material. The useful life of a polycrystalline material is limited by the combined effects of these micromechanistic processes. It is therefore important to identify and evaluate the nature and development of the damage accumulation which leads to failure. Knowledge of the operational damage could be useful in a number of ways; it would provide an understanding of the behaviour of the material in service conditions and hence contribute to more reliable design performance.

In the present investigation we aim at determining combined effects of stress deformation and fracture characteristics of the conventionally cast (CC) MAR-M 002 superalloy.

2. Experimental procedure

The material used in the present study is a commercial nickel-based superalloy, MAR-M 002, of composition 2.5 wt% Ta, 10 wt% W, 9.0 wt% Cr, 5.5 wt% Al, 1.5 wt% Ti, 10 wt% Co, 1.5 wt% Hf, 0.05 wt% Zr, 0.14 wt% C, 0.015 wt% B and balance nickel. In order to produce a variety of microstructural distributions, including grain morphology, γ' phase and carbide dispersions, the creep specimens were deliberately cast to shape at different solidification rates. After casting, the creep specimens were machined to 4 mm gauge diameter. Creep testing was carried out to failure at 1173 K (900 °C) using a uniaxial constant load in air. Stresses ranging from 200 to 400 MPa were applied to creep specimens. The temperature was kept constant within $\pm$ 0.5 K. The creep elongation was recorded continuously using differential transformers. For the cavity measurements, Six scanning electron cavity micrographs with adjoining fields from the gold-coated samples were taken from the entire cross-sections of fractured specimens. The Cambridge Instruments Q-520 system was used for the quantitative evaluations of the cavity size (mean surface area, S), number of cavity per cross-section (cavity density, N_A, and cavity volume fraction, f_c). The linear mean cavity size, a_c, was evaluated as the square root of the mean cavity area (i.e., $S^{1/2}$), whereas the intercavity spacing, L, was determined using the following formula: $L = 0.5/N_A^{1/2}$.

3. Results and discussion

3.1. Fracture cavitation

A quantitative assessment of the kinetics of intergranular cavity damage accumulation was carried out on fractured specimens. Fig. 1 shows the effect of applied stress on the cavity volume fraction, f_c; there is

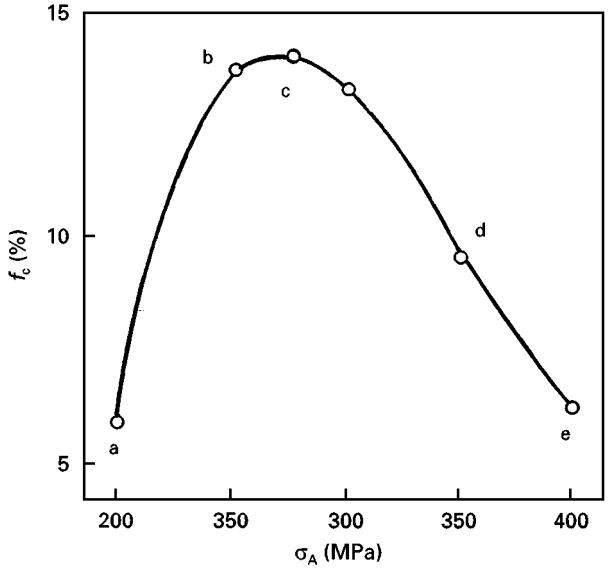

Figure 1 Effect of applied stress, σ_A, on the cavity volume fraction, f_c.

a maximum in the curve. Different cavity morphologies as a function of stress are given in Fig. 2. These micrographs indicate that the cavity morphologies exist as the round type cavities (i.e., Fig. 2a and e) and the dendritic shape cavities (i.e., Fig. 2c); these cavities are usually associated with the eutectic pools. The cavity shapes become more dendritic when their volume fraction increases (from point a through b to point c or from point e to point d in Fig. 1 (i.e., Fig. 2a → Fig. 2b → Fig. 2c or e → Fig. 2d).

3.2. Creep life predictions

3.2.1. Parametric approach

Cavity nucleation is dependent both on strain and on stress level. Several workers [6–10] have proposed that cavity nuclation rate, $\dot{N}_A$, is directly proportional to the creep rate, $\dot{\varepsilon}$, i.e., $\dot{N}_A = K_1\dot{\varepsilon}$, where K_1 is the nucleation rate coefficient dependent primarily on the density of carbides [11]. The above expression can be integrated with respect to time which leads to an expected linear dependence of cavity density, N_A, with creep strain, ε_R, i.e., $N_A = K_1\varepsilon_R$, assuming that the rate of nucleation is constant with time. Therefore, on the basis of above discussion, and as in the literature [6–10], it is assumed that the cavity density, N_A, may be expressed by the functional relation

$$N_A = f(\varepsilon_R,\ t_R,\ \sigma_A) \tag{1}$$

or

$$N_A = K\varepsilon_R t_R \sigma_A^m \tag{2}$$

where ε_R is the creep rupture strain, t_R is the creep rupture life, σ_A is the applied stress, and K and m are constants.

The cavity density, N_A, is plotted against the $\varepsilon_R t_R \sigma_A^4$ product as shown in Fig. 3 which reveals quite a good linear correlation. A parametric approach of this type can be used satisfactorily by assuming a stress exponent of $m = 4$ [6, 9]. The fact that the number, N_A, of cavities can be correlated with the rupture strain, time and stress implies that cavity nucleation is controlled by the same mechanism that is controlling creep deformation and fracture processes. Futhermore, Equation 2 gives the relative contribution of each variable to the creep damage, N_A, independently of the effect of the other variables. The linear correlation between N_A and $\varepsilon_R t_R \sigma_A^4$ (Fig. 3) indicates that the nucleation of cavity appeared to start right after loading and proceeded steadily through all creep stages, and that it is the cavity growth process which dominantly affected creep rupture life, t_R. In the past, a linear relationship has been observed between the cavity volume fraction, f_c, and the $\varepsilon_R t_R \sigma^m$ product for a number of single-phase materials [12–14] and engineering alloys [15–16]. The stress exponent m was 7.5 for pure nickel, which indicates the difference between the behaviours of pure nickel and commercial nickel-based alloys such as IN-100 [16] and present alloy.

3.2.2. Creep crack growth approach

Several reports exists in the literature of the application of elasto-plastic fracture mechanics to describe intergranular creep fracture [17]. Intergranular creep fracture is a multiple-crack-growth and interlinkage fracture mode which involves plastic deformation. In an attempt to modify elasto-plastic fracture mechanics to describe such a fracture mode an empirical stress-intensity factor, K_{CR}, approach has been introduced [18, 19]. The theory of elasto-plastic fracture mechanics cannot be directly applied to creep fracture and in order to clarify the situation it was proposed [20] that the stress-intensity factor, K_{CR}, should simply be called a rupture parameter, K_f, which makes no claims to be a measure of stress, σ_A, or strain in front of an advancing crack tip. The rupture parameter, K_f, is purely empirical and calculated on the basis of Equation 5 but will be shown to be of value in the prediction of creep rupture life, t_R.

Measurements of the crack velocity $\dot{a}$ during creep rupture reveal that it varies with the applied stress-intensity factor, K, in the form of a power law [21, 22]

$$\dot{a} = B K^m \tag{3}$$

where B is a constant that depends exponentially on temperature, and the exponent m takes value between 1 and 6 [23, 24] although vastly higher values have been reported [25] but for a particular material is usually close to the value of the stress exponent, n, of minimum creep rate, $\dot{\varepsilon}_m$, in power-law creep: $\dot{\varepsilon}_m \propto \sigma_A^n$. The crack velocity $\dot{a}$ is therefore strongly dependent on both the stress-intensity factor and the temperature. Therefore, the stress intensity factor, K, has sometimes been used in the past to characterize the creep crack growth (CCG) (or crack velocity), $\dot{a}$, under small-scale creep conditions.

In the present study, on the basis of the previous discussion given above a modified Griffith–Irwin type of relation is used to investigate the influence of the applied stress on the cavity (microcrack) size, a_c, to produce final crack propagation. The plot of cavity size, a_c, observed in each specimen against the applied

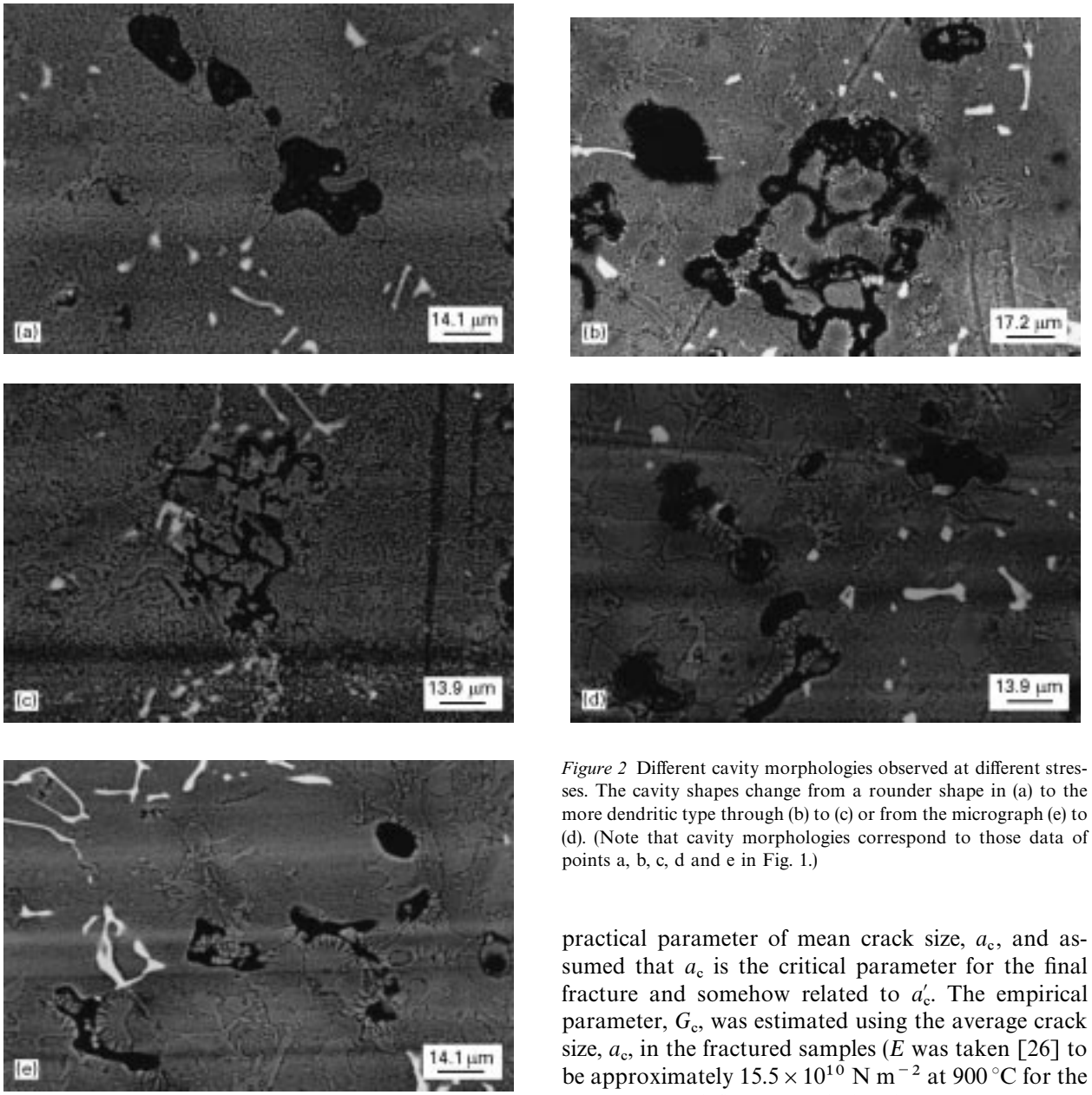

Figure 2 Different cavity morphologies observed at different stresses. The cavity shapes change from a rounder shape in (a) to the more dendritic type through (b) to (c) or from the micrograph (e) to (d). (Note that cavity morphologies correspond to those data of points a, b, c, d and e in Fig. 1.)

stress, σ_A, is shown in Fig. 4 in terms of the Equation.

$$\sigma_f \propto \left(\frac{EG_c}{\pi a_c}\right)^{1/2} \tag{4}$$

where σ_f is the applied stress for fracture (or σ_A), E is Young's modulus and G_c is an empirical parameter related to the energy release rate. The decrease in crack size with increase in stress level (Fig. 4) indicates that crack growth past a GB carbide particle is difficult. This variation in crack size with stress is to be expected since the time for cracks to grow into final crack size increases with a decrease in stress level [5, 13]. We can rewrite Equation 4 as follows:

$$K_f \propto \sigma_f\left(\pi a_c'\right)^{1/2} \tag{5}$$

where $K_f = (EG_c)^{1/2}$ is called an empirical rupture parameter (or the creep-fracture parameter), and a_c' is the maximum crack size. Since it is not possible to determine a_c' reliably we have used a more reliable and practical parameter of mean crack size, a_c, and assumed that a_c is the critical parameter for the final fracture and somehow related to a_c'. The empirical parameter, G_c, was estimated using the average crack size, a_c, in the fractured samples (E was taken [26] to be approximately 15.5×10^{10} N m^{-2} at 900 °C for the present material). The variation in G_c suggests that various microstructural parameters such as the grain size, GB carbide particles, and the cavitation, affect it. In fact, the effect of microstructure such as the cavitation density, N_A, on G_c is shown in Fig. 5. As the logarithmic plot of G_c against N_A indicates in this figure the following type of correlation exists between G_c and N_A:

$$G_c \propto \frac{1}{N_A^{1/3}} \tag{6}$$

Previous work [11] showed that there was a direct correlation between the cavity and GB carbide particle densities for the present material. Therefore, it is suggested that decreasing the carbide particle density (number of carbide particles per unit area) increases the empirical parameter, G_c, related to fracture the GB carbide-matrix surface area (decohesion).

A plot of the creep-fracture parameter, K_f, against the creep rupture life, t_R, is illustrated in Fig. 6, which yields the following type of relationship:

$$K_f \propto \frac{1}{t_R^{3.6}} \tag{7}$$

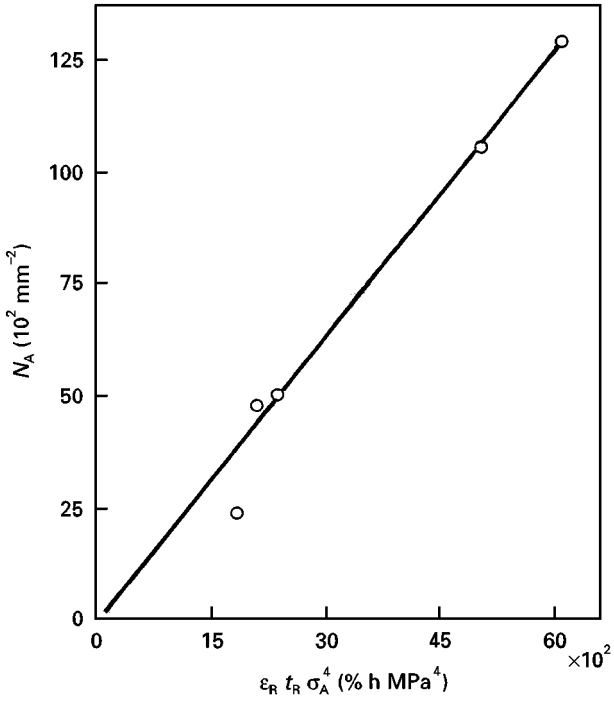

Figure 3 Linear dependence of the cavity population, N_A, on the ε_R t_R σ_A^4 product.

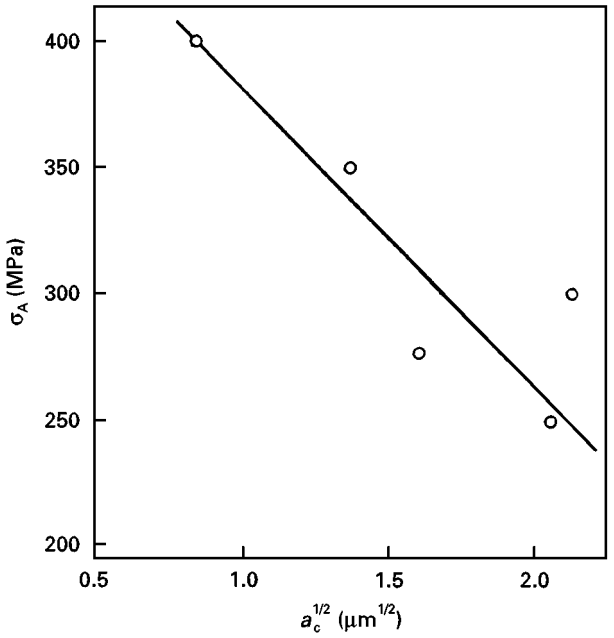

Figure 4 Inverse linear dependence of the crack size, a_c, on the applied stress, σ_A.

Therefore, the empirical rupture parameter approach, K_f, can be used to predict t_R. The exponent for K_f is close to the effective stress exponent (i.e., $n = 4$) in power-law creep in nickel-based superalloys [27]. This suggests that the cavity growth process is somehow related to the PLC [25] which supports the previous findings (see Equation 3). From Equations 3 and 7 it is suggested that accelerating the CCG rate (or crack velocity $\dot{a}$) increases the creep-fracture parameter, K_f, and in turn causes the creep rupture life, t_R, to deteriorate.

From the cavities observed after creep fracture the total length of damaged GB (or the GB damage accumulation), L_T, was calculated to investigate the effect of the damage accumulation on t_R:

$$L_T = N_A a_c \tag{8}$$

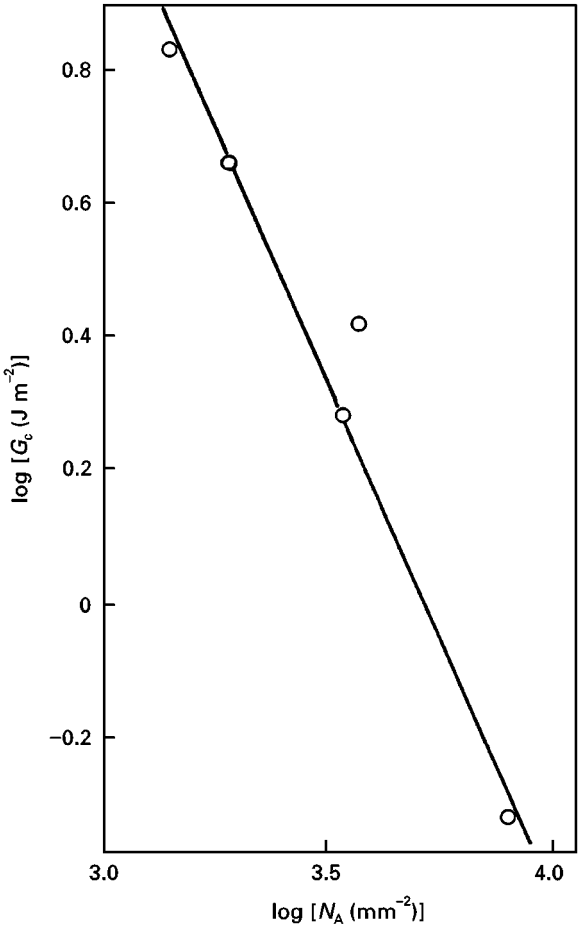

Figure 5 Inverse linear dependence of G_c on N_A on a log–log scale.

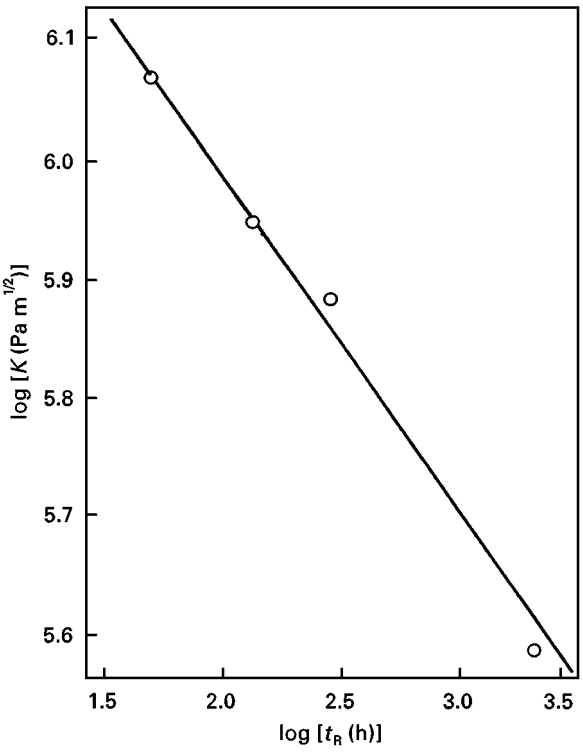

Figure 6 Inverse linear dependence of the creep-fracture parameter, K_f, on the creep rupture life: $K_f \propto t_R^{-1/3.6}$.

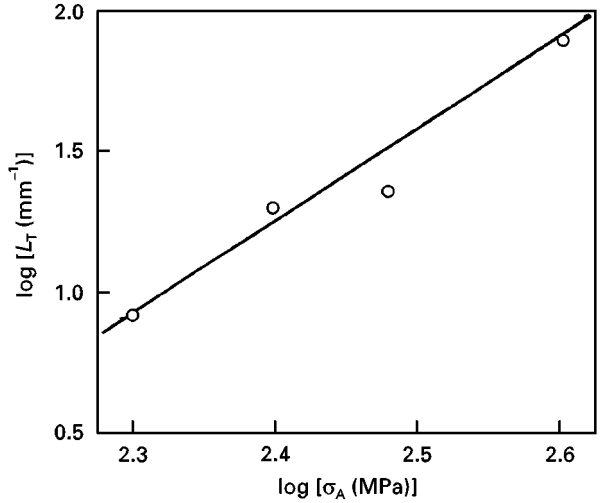

Figure 7 Effect of the applied stress on the damage accumulation, L_T.

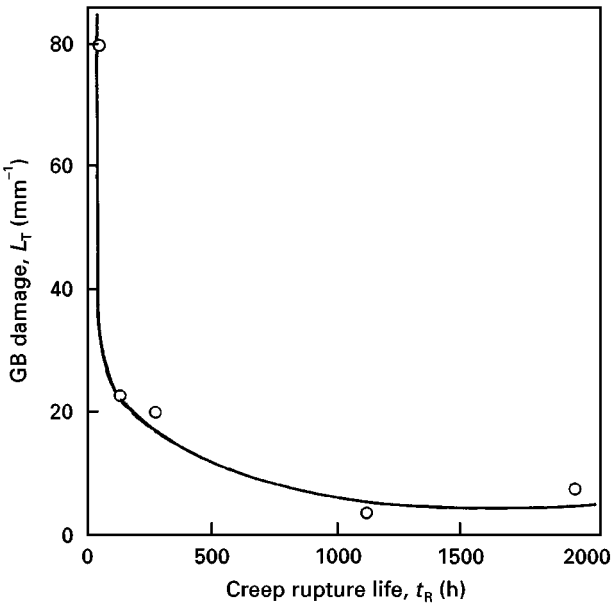

Figure 8 Influence of the damage accumulation, L_T, on the creep rupture life.

The GB damage accumulation, L_T, was plotted against the applied stress, σ_A, as shown in Fig. 7, indicating that the extent of damage increases with an increase in stress in the following way:

$$L_T \propto \sigma_A^{3.3} \tag{9}$$

This relationship indicates that the extent of damage is reasonably sensitive to the stress. Fig. 8 shows the influence of the GB damage, L_T, on the creep rupture life, which indicates that decreasing the GB damage accumulation first slowly increases t_R down to a critical value of L_T and further, on decreasing L_T below that value ($\approx$ about 20 mm^{-1}), t_R improves sharply.

3.2.3. Coupled power-law creep and grain-boundary diffusion mechanism approach

The size and spacing of the cavities is such that cavity growth is expected to be controlled by the coupling of GB diffusion and PLC. The rupture properties of these samples were studied over a range of stresses and the results are compared with the predictions of various theoretical treatments of cavity growth.

The fracture process includes the nucleation and growth of creep cavities, the coalescence of cavities into microcracks, the interlinkage of microcracks to form a macroscopic crack and propagation of a macroscopic crack across the components, leading to the ultimate fracture. Among these steps, creep cavity growth is usually the rate-controlling steps and hence has been the subject of extensive study for the past three decades. Creep cavitation can grow by mechanisms controlled by GB diffusion, by surface diffusion, by PLC, and by any combination of two of these mechanisms. The problem of coupling diffusive cavity growth with PLC has been analysed by different workers [1–4]. It was suggested by these workers that the GB area between cavities should be divided into two regions: one which is adjacent to the cavities, where GB diffusion occurs, and the other which is midway between the cavities, where PLC occurs. Needleman and Rice [3] attempted to solve the problem of coupled cavity growth by diffusion and PLC exactly in terms of a stress and temperature-dependent "material length scale" or characteristic diffusion length, Λ:

$$\Lambda = \left(\frac{D_B \delta_B \Omega \sigma_\infty}{(kT\dot{\varepsilon}} \right)^{1/3} \tag{10}$$

where D_B (m^2 s^{-1}) is the GB diffusion rate constant, δ_B (m) the GB width, Ω (m^3) the atomic volume, σ_∞ (or σ_A) the applied stress, k Boltzmann's constant (equal to 1.38×10^{-23} J K^{-1}), T the absolute temperature and $\dot{\varepsilon}_\infty$ the remote creep rate (or minimum creep rate, $\dot{\varepsilon}_m$). The contribution of dislocation creep (i.e., PLC) to cavity growth is shown to be negligible when $\Lambda > L$. Significant interaction occurs when $\Lambda < L$. Edward and Ashby [2] determined the size of the diffusional zone by the dimensionless parameter P^*:

$$P^* = \frac{1}{10} \left(\frac{4\Lambda^3}{L^3} \right)^{2/n} \tag{11}$$

This parameter, P^*, is also useful for the determination of which mode of cavity growth mechanism dominates the creep life under various creep conditions. It was predicted [2] that, for $P^* \geqslant 1$ (i.e., larger values of length parameter or small cavity spacings, L), there is a negligible contribution of PLC to cavity growth and rupture process is controlled by the GB diffusion. When $P^* \leqslant 10^{-3}$, the diffusional growth contributes negligibly and PLC dominates. Within the above two bounds of P^*, (i.e., $10^{-3} < P^* < 1$), both the diffusional and the PLC growth contributions are important in determining the creep rupture life, t_R.

Using the following material constants [5] for MAR-M 002 alloy the values of Λ and P^* were calculated for various $\dot{\varepsilon}_m$ and L values observed in the present investigation for MAR-M 002 alloy tested at various stress levels, σ_A or σ_∞:

$$\delta_{0B} D_{0B} = 2.8 \times 10^{-15} \text{m}^3 \text{ s}^{-1}$$

$$\Omega = 1.1 \times 10^{-29} \text{m}^3$$

$$Q_B = 115 \text{ kJ mol}^{-1}$$

TABLE I Data for Λ and P^* calculated under various creep conditions (P^* was calculated using Equation 11)

Specimen	σ_A (MPa)	Λ (μm)	L (μm)	P^*
1	200	130	1.4	181
2	250	69	7.3	5.8
3	275	145	12.8	7.6
4	300	267	7.1	46.3
5	350	37	3.4	7.3
6	400	27	1.5	15.6

where $\delta_{0B} D_{0B}$ is the pre-exponential term for the GB diffusion constant, Q_B is the activation energy for GB diffusion and n is taken to be the effective stress exponent ($n = 4$) in $\dot{\varepsilon}_m \propto \sigma_A^n$ [27]. Note that $\delta_B D_B$ was calculated using the following Arrhenius-type equation [28]:

$$\delta_B D_B = \delta_{0B} D_{0B} \exp\left(-\frac{Q_B}{RT}\right) \tag{12}$$

with R the gas constant (8.31 J mol^{-1} K^{-1}).

Under the present creep conditions ($T = 1173$ K; $\sigma_\infty = 200$–400 MPa) depending on the observed values of L and $\dot{\varepsilon}_\infty$ (or $\dot{\varepsilon}_m$) for various values of applied stress the following values of Λ and P^* (as given in Table I) were determined:

$$\Lambda \approx 27\text{–}270\ \mu\text{m}\ (> L \approx 1.5\text{–}13\ \mu\text{m});\ P^* \approx 7\text{–}180 > 1.$$

These numerical calculations suggest that there is a negligible contribution of creep flow (or PLC) to cavity growth, and so the rupture process in CC MAR-M 002 under the present creep conditions is predicted to be controlled by GB diffusion mechanism. Cocks and Ashby [5] have given the approximate analytical equation for the time to rupture, t_R, under a constant-load condition for the GB diffusion mechanism alone as

$$t_R = t_n + \frac{2}{3\Phi_0 \dot{\varepsilon}_0}\left\{f_c^{3/2}\left[\ln\left(\frac{1}{f_c}\right) + \frac{2}{3}\right] - f_i^{3/2}\left[\ln\left(\frac{1}{f_i}\right) + \frac{2}{3}\right]\right\}\frac{\sigma_0}{\sigma_1} \tag{13}$$

where t_n is the time to nucleate a void (or cavity), Φ_0 the dimensionless quantity which appears when GB diffusion and PLC are coupled, $\dot{\varepsilon}_0$ (s^{-1}) the creep constant, f_i the initial area fraction of cavity holes, σ_0 the mean stress in damaged region when cavities are heterogeneously distributed and σ_1 the principal stress. Φ_0 is defined [5] as the material property, by

$$\Phi_0 = \frac{2\delta_B D_B \Omega}{kTL^3}\frac{\sigma_0}{\sigma_1} \tag{14}$$

Neglecting t_n and f_i (because these terms are generally small) and assuming the other factors (i.e., δ_B, D_B, $\dot{\varepsilon}_0$ and σ_0) in Equations 13 and 14 to be constant, then Equation (13) can be written as

$$t_R \propto \frac{L^3 f_c^{3/2}}{\sigma_A}\left(\frac{2}{3} - \ln(f_c)\right) = B \tag{15}$$

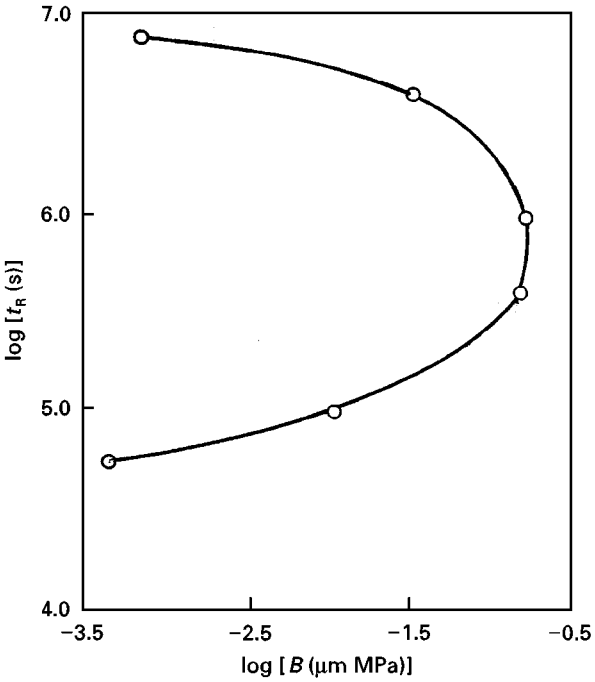

Figure 9 The plotting of the observed creep rupture life against the calculated parameter, B (Equation 15) when the cavity growth is controlled by the GB diffusion mechanism.

(Note that, for polycrystalline materials, σ_1 may be taken to be equal to $\sigma_A/2$). Equation 15 indicates that the creep rupture life is propotional to the parameter, B, for the GB diffusion mechanism. Fig. 9 gives the plotting of the observed creep rupture life, t_R, against the calculated parameter, B, according to equation 15 which indicates a complicated relationship. Therefore, from Fig. 9 it is clearly seen that the operational cavity growth mechanism in the tertiary creep region is not the GB diffusion mechanism.

To predict the cavity growth mechanism in the tertiary creep region the dimensionless parameter, P^*, was recalculated using the following expression [2]:

$$P^* = \frac{1}{10}\left[2\Phi_0'\left(\frac{\sigma_0}{\sigma_1}\right)^{n-1}\right]^{2/n} \tag{16}$$

where σ_0(N m^{-2}) is the creep constant and n the stress exponent in the PLC expression (n was taken to be 4). Φ_0' is defined [2] as the important material property, by

$$\Phi_0' = \beta f_c^{3/2} \ln\left(\frac{1}{f_c}\right)\left(\frac{1}{(1-f_c)^n} - (1-f_c)\right)\left(\frac{\sigma_e}{\sigma_0}\right)^n \frac{\sigma_0}{\sigma_1} \tag{17}$$

For the numerical calculations of Φ_0' the result for simple tension as in the present case was obtained [2] by setting $\beta = 0.6$ and $\sigma_e = \sigma_1$ (where σ_e is the equivalent tensile stress). For polycrystalline materials, σ_1 may be taken to be equal to $\sigma_A/2$. The constant σ_0 was taken [3] to be 4097×10^6 N m^{-2}. Using the experimental cavity parameter, f_c, and various applied stresses, σ_A in each creep test the parameter, P^*, (Equation 16) was found to vary between about 20×10^{-3} and about 35×10^{-3} (i.e., $1 > P^* > 10^{-3}$). (Data for P^* for various creep test conditions are

TABLE II Modified version of P^* (using Equation 16)

Specimen	σ_A (MPa)	$\Phi'_0 \times 10^6$	$P^* \times 10^3$
1	200	2.00	18.6
2	250	12.0	32.5
3	275	16.5	33.0
4	300	19.8	31.7
5	350	20.4	25.6
6	400	17.1	19.2

given in Table II). These results for the P^* parameter indicates that the creep fracture cavity growth is controlled by the coupled PLC with the GB diffusion mechanism. Cocks and Ashby [5] have also given an approximate analytical equation for the rupture time, t_R, under the constant-load condition for coupled GB diffusion and PLC as

$$t_R = t_n + \frac{2}{3}\frac{(f_t^b)^{3/2}}{\Phi'_0\dot{\varepsilon}_0}\left(\ln\left(\frac{1}{f_t^b}\right)+\frac{2}{3}\right)\frac{\sigma_0}{\sigma_1} + \frac{1}{[\beta(n+1)\dot{\varepsilon}_0]} \times \ln\left(\frac{1}{(n+1)f_t^b}\right)\left(\frac{\sigma_0}{\sigma_e}\right)^n \quad (18)$$

where f_t^b is the area fraction of cavity holes at transition from growth by GB diffusion to PLC growth in approximate analysis, $\dot{\varepsilon}_0$ (s^{-1}) is the creep constant, and σ_e is the von Mises equivalent stress and is taken to be the axial stress σ_1 (or σ_A) in simple tension. The critical area fraction, f_t^b, at which the change in mechanism from the GB diffusion to the PLC occurs can be solved [2]:

$$f_t^b = \frac{1}{[d(\ln d - 1)]^{3/2}} \quad (19)$$

where

$$d = \frac{4(n+1)}{3\Phi'_0}\left(\frac{\sigma_e}{\sigma_0}\right)^n \frac{\sigma_0}{\sigma_1}\beta \quad (20)$$

The creep rupture life, t_R, predicted using Equation 18 depends on the quantity Φ'_0 and on the applied stress σ_A. For the prediction of the creep rupture life using Equation 18 the following constants were used for various applied stress ($\sigma_A = 200$–400 MPa) and observed cavity parameter, f_c: $\sigma_0 \approx 4097 \times 10^6$ N m^{-2} [3]; $\dot{\varepsilon}_0 = 2.627 \times 10^{-10} s^{-1}$ [3]; $\beta = 0.6$ [5]; $\sigma_e = \sigma_1 = \sigma_A$; $n = 4$; $t_n = 0$ (assumed).

The predicted creep rupture lives using Equation 18 were plotted against the observed values, as illustrated in Fig. 10. As can be seen in this figure, the prediction of the time, t_R, based on the coupled GB diffusion and PLC shows, however, that Equation 18 results in a time that is almost twice the actual creep rupture life, indicating that a better theoretical model is required that accounts for the gradual accumulation of damage. (In Equation 18 all the cavities are assumed [5] to nucleate at a strain, ε_n (corresponding to t_n).) In simple tension, it was shown [2] that, at one limit (low Φ'_0; large σ_A), the creep life reduces to the value calculated for GB diffusion alone (Equation 13 or 15); at the other limit it reduces to the result for power-law creep alone (Equation 20 or 21). Therefore, it is interesting

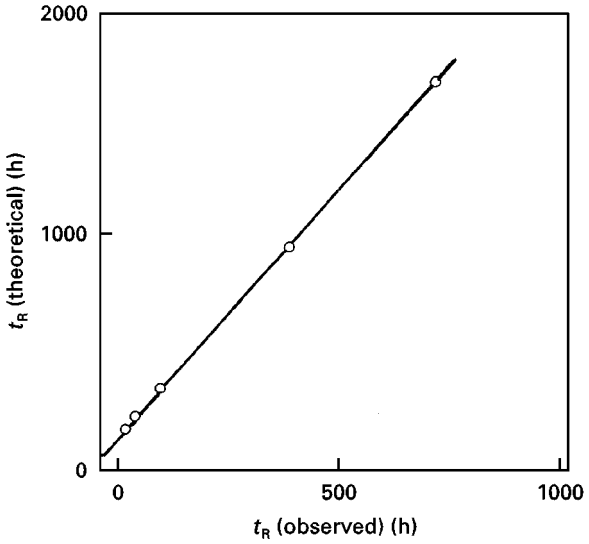

Figure 10 Linear correlation between the observed creep rupture lives and the calculated values using the coupled mechanism between the GB diffusion and PLC (Equation 18).

to predict the contributions of each of these mechanisms. The following relation was developed for the PLC mechanism [5]:

$$t_R = t_n + \frac{1}{\beta(n+1)\dot{\varepsilon}_0}\ln\left(\frac{1-(1-f_c)^{n+1}}{1-(1-f_i)^{n+1}}\right)\left(\frac{\sigma_0}{\sigma_e}\right)^n \quad (21)$$

Assuming that $t_n = 0$, that the parameters β, $\dot{\varepsilon}_0$ and σ_0 constant, that f_i equals a very small value, that $n = 4$ and that $t_R \propto 1/\sigma_A$ on a log–log scale [29], then Equation 21 becomes

$$t_R \propto \sigma_A^4 \ln[1-(1-f_c)^5] = A \quad (22)$$

The relative contribution of PLC to the overall creep rupture life was calculated using "A" in Equation 22, and that the observed creep rupture life was plotted against A, as seen in Fig. 11. This plot indicates that increasing the PLC contribution above a critical value increases the creep rupture life sharply. The relative contribution of the GB diffusion and PLC mechanisms were also predicted by establishing the A/B ratio. Fig. 12 illustrates the plot of creep rupture life against this ratio; decreasing this ratio (increasing the GB diffusion contribution and decreasing the PLC contribution) continuously improves the creep rupture life. From the slopes of this curve at various points it is concluded that the GB diffusion contribution rate is approximately four orders higher at point D compared with that at point E.

4. Summary and conclusions

Analysis of material fracture frequently considers the initiation and propagation of cracks and the final failure as three individual steps. Each step can be analysed separately. For the prediction of the creep life the growth of intergranular creep cavities has been studied in CC MAR-M 002 alloy tested at 900 °C over a limited range of stress ($\sigma_A = 200$–400 MPa). The creep rupture life can be improved sharply by

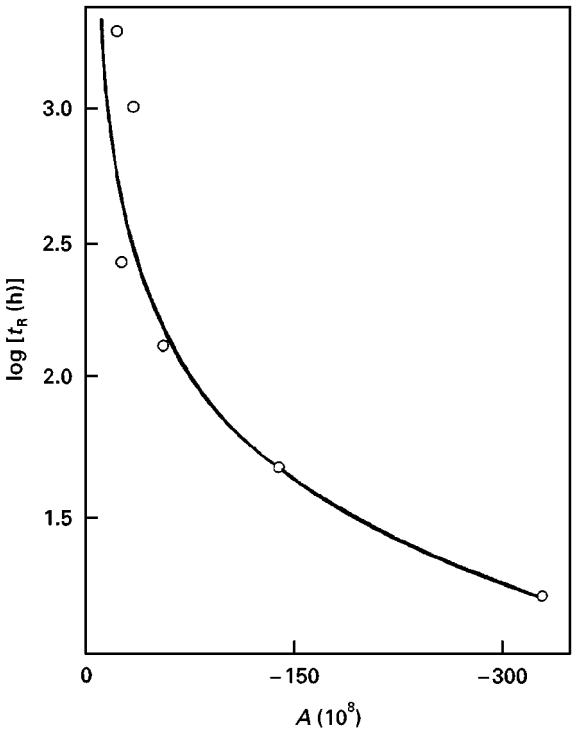

Figure 11 Contribution of the PLC creep to the creep rupture life, t_R, increases with increasing "A".

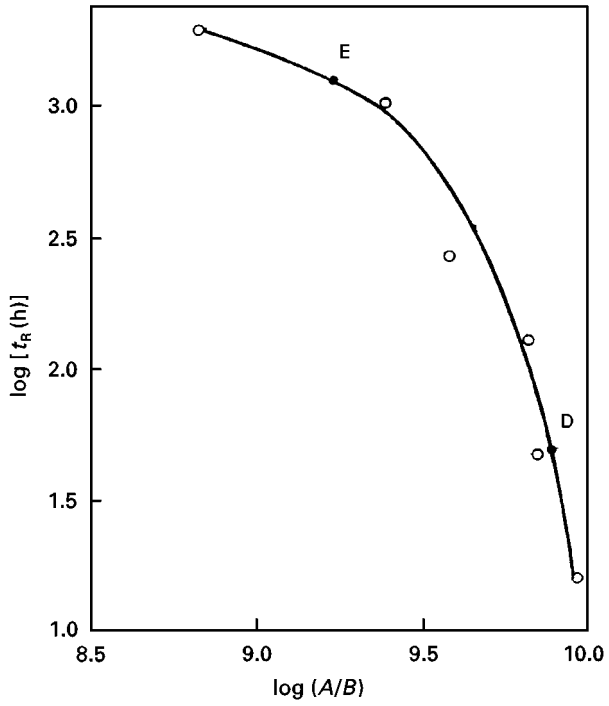

Figure 12 Relative contributions of the PLC and the GB diffusion mechanisms to the creep rupture life.

decreasing the GB damage, L_T, below its critical value (about 20 mm^{-1}). The non-linear dependence of t_R on the diffusion parameter, B (Fig. 9), indicates that a GB diffusion-controlled process in the tertiary region can be discounted. In fact, the coupled PLC with GB diffusion mechanism was predicted to be operative in the tertiary region. In the present work, two different approaches have been used for the prediction of creep rupture life, t_R: firstly empirical approach; secondly the cavity growth mechanism (approach) that controls the fracture process. It was found that the number, N_A, of cavities per unit area is linearly related to the time-dependent creep strain ε_R, stress, σ_A, and creep rupture life, t_R, through the $\varepsilon_R\ t_R\ \sigma_A^4$ parameter. Therefore, using the cavity population (cavity density) and this parameter the creep rupture life can be predicted reasonably well.

Another empirical approach, is the simple creep fracture parameter, K_f, developed using the modified Griffith–Irwin type of relationship, which can be used to predict the creep rupture life. The fact that in $K_f \propto t_R^{-3.6}$ relationship the exponent of rupture life is quite close to the effective stress exponent in the PLC (i.e., $n = 4$) suggests that the creep rupture process in the tertiary creep region is somewhat related to the PLC in the secondary creep region.

Edward and Ashby [2] have proposed a model which explicitly yields equations for t_R governed by either PLC or by a coupled GB diffusion–PLC process. Because of the simplified constitutive laws used to describe creep deformation and diffusive growth, these solutions only approximate the physical processes occurring [2, 5]. In the coupled growth model developed by Edward and Ashby, which is the predicted operational cavity growth model in the present conditions, the material diffused from the internal cavity surface is accommodated by creep deformation (PLC) of the matrix adjoining the cavity. This shortens the effective diffusion path length and results in a faster rate of cavity (i.e., decreased t_R) than would occur by either GB diffusion or PLC alone. In fact, as shown in Fig. 11, when the PLC contribution to the GB diffusion increases, the creep rupture life continuously decreases as a result of the increased GB damage accumulation, L_T (Fig. 8). The linear correlation between predicted and observed creep rupture life (Fig. 10) indicates that the main factor controlling the life of a material, when failure is an intergranular process (controlled by GB diffusion and PLC), is the cavity growth. Thus, it is imperative that factors controlling cavity growth mechanism be identified first. However, this prediction based on the coupled GB diffusion and PLC overestimates the time, t_R, indicating that a more refined model is required that accounts for the gradual accommodation and shape of cavities.

References

1. W. BEERE and M. V. SPEIGHT, *Metal Sci.* **12** (1978) 172.
2. G. H. EDWARD and M. F. ASHBY, *Acta Metall.* **27** (1979) 1505.
3. A. NEEDLEMAN and J. R. RICE, *ibid.* **28** (1980) 1315.
4. I. W. CHEN and A. S. ARGON, *ibid.* **29** (1981) 1759.
5. A. C. F. COCKS and M. F. ASHBY, *Progr. Mater. Sci.* **27** (1982) 189.
6. B. J. CANE and G. W. GREENWOOD, *Metal Sci.* **9** (1975) 55.
7. B. F. DYSON and D. MCLEAN, *ibid.* **11** (1977) 37.
8. I. W. CHEN and A. S. ARGON, *Acta Metall.* **29** (1981) 1321.
9. B. J. CANE, *Metal Sci.* **12** (1978) 102.
10. M. A. CAPANO, A. S. ARGON and I. W. CHEN, *Acta Metall.* **37** (1989) 3195.
11. A. BALDAN, *Z. Metallkd.* **85** (1994) 400.
12. D. A. WOODFORD, *Metal Sci. J.* **3** (1969) 50.
13. N. G. NEEDHAM, J. E. WHEATLEY and G. W. GREENWOOD, *Acta Metall.* **23** (1975) 23.

14. D. A. WOODFORD, *Metal Sci. J.* **3** (1969) 234.
15. N. G. NEEDHAM and T. GLADMAN, *ibid.* **14** (1980) 64.
16. A. BALDAN, *Phys. Status. Solidi.* (*a*) **128** (1991) 383.
17. C. E. TURNER and G. A. WEBSTER, *Int. J. Fracture* **10** (1974) 455.
18. P. K. VENKITESWARAN and D. M. R. TAPLIN, *Metal Sci.* **8** (1974) 97.
19. V. KUTUMBA RAO, D. M. R. TAPLIN and P. RAMA RAO, *Metall. Trans. A* **6** (1975) 77.
20. R. G. FLECK, C. J. BEEVERS and D. M. R. TAPLIN, *Metal Sci.* **10** (1976) 413.
21. G. J. NEATE and M. J. SIVERNS, in Proceedings of the International Conference on Creep and Fracture in Elevated Temperature Applications (Institution of Mechanical Engineers, London, 1973–4.
22. K. M. NIKBIN, G. A. WEBSTER and C. E. TURNER, in "Fracture 1977", Proceedings of the Fourth International Conference on Fracture Vol. 2, Waterloo, Ontario 19 –24 June, 1977 (Pergamon, Oxford, 1977 pp. 627).
23. K. JAKUS, S. M. WIEDERHORN and B. J. HOCKEY, *J. Amer. Ceram. Soc.* **69** (1986) 725.
24. A. G. EVANS and S. M. WIEDERHORN, *J. Mater. Sci.* **9** (1974) 270.
25. B. S. B. KARUNARATNE and M. H. LEWIS, *ibid.* **15** (1980) 449.
26. H. A. KUHN and H. G. SOCKEL, *Mater. Sci. Engng* **A 112** (1989) 117.
27. J. P. DENNISON, P. D. HOLMES and B. WILSHIRE, *ibid.* **33** (1978) 35.
28. H. J. FROST and M. F. ASHBY, "Deformation mechanism maps, the plasticity and creep of metals and ceramics" (Pergamon, Oxford, 1982) p. 55.
29. A. BALDAN, Unpublished work.

Received 20 May 1997
and accepted 11 May 1998